Renal function support with *Phyllanthus niruri* (Chanca Piedra)

The following studies observed the effect of *P. niruri* on protecting renal tissue and preserving renal function in patients with urinary stones.

frontiers | Frontiers in Pharmacology

ORIGINAL RESEARCH
published: 16 June 2022
doi: 10.3389/fphar.2022.891788

Phyllanthus Niruri L. Exerts Protective Effects Against the Calcium Oxalate-Induced Renal Injury *via* Ellgic Acid

Mao-Ting Li[1†], Lu-Lu Liu[1†], Qi Zhou[1†], Lin-Xi Huang[1], Yu-Xuan Shi[1], Jie-Bin Hou[2], Hong-Tao Lu[3], Bing Yu[4], Wei Chen[1] and Zhi-Yong Guo[1*]*

[1]Changhai Hospital, Naval Medical University, Shanghai, China, [2]Department of Nephrology, the Second Medical Centre, Chinese PLA General Hospital, Beijing, China, [3]Department of Naval Medicine, Naval Medical University, Shanghai, China, [4]Department of Cell Biology, Center for Stem Cell and Medicine, Navy Medical University, Shanghai, China

Background: Urolithiasis or kidney stones is a common and frequently occurring renal disease; calcium oxalate (CaOx) crystals are responsible for 80% of urolithiasis cases. *Phyllanthus* niruri L. (PN) has been used to treat urolithiasis. This study aimed to determine the potential protective effects and molecular mechanism of PN on calcium oxalate-induced renal injury.

Methods: Microarray data sets were generated from the calcium oxalate-induced renal injury model of HK-2 cells and potential disease-related targets were identified. Network pharmacology was employed to identify drug-related targets of PN and construct the active ingredient-target network. Finally, the putative therapeutic targets and active ingredients of PN were verified *in vitro* and *in vivo*.

Results: A total of 20 active ingredients in PN, 2,428 drug-related targets, and 127 disease-related targets were identified. According to network pharmacology analysis, HMGCS1, SQLE, and SCD were identified as predicted therapeutic target and ellagic acid (EA) was identified as the active ingredient by molecular docking analysis. The increased expression of SQLE, SCD, and HMGCS1 due to calcium oxalate-induced renal injury in HK-2 cells was found to be significantly inhibited by EA. Immunohistochemical in mice also showed that the levels of SQLE, SCD, and HMGCS1 were remarkably restored after EA treatment.

Conclusion: EA is the active ingredient in PN responsible for its protective effects against CaOx-induced renal injury. SQLE, SCD, and HMGCS1 are putative therapeutic targets of EA.

Keywords: *Phyllanthus* niruri L., calcium oxalate-induced renal injury, network pharmacology, ellagic acid, lipid nephrotoxicity

OPEN ACCESS

Edited by:
Ying-Yong Zhao,
Northwest University, China

Reviewed by:
Jiaqiao Zhang,
Huazhong University of Science and Technology, China
Zongyao Hao,
Anhui Medical University, China

***Correspondence:**
Wei Chen
wujiang02@163.com
Zhi-Yong Guo
drguozhiyong@163.com

[†]These authors have contributed equally to this work and share first authorship

Specialty section:
This article was submitted to Renal Pharmacology, a section of the journal Frontiers in Pharmacology

Received: *08 March 2022*
Accepted: *11 May 2022*
Published: *16 June 2022*

Citation:
Li M-T, Liu L-L, Zhou Q, Huang L-X, Shi Y-X, Hou J-B, Lu H-T, Yu B, Chen W and Guo Z-Y (2022) Phyllanthus Niruri L. Exerts Protective Effects Against the Calcium Oxalate-Induced Renal Injury via Ellgic Acid. Front. Pharmacol. 13:891788. doi: 10.3389/fphar.2022.891788

1 INTRODUCTION

Phyllanthus niruri L. (PN) belongs to *Phyllanthus* Linn., Subgen. *Phyllanthus*, Sect. *Phyllanthus* and the species *Phyllanthus* niruri. It is distributed in China, India, Indochina Peninsula, Malay Archipelago, and tropical America (China Plants Database, http://db.kib.ac.cn/CNFlora/HierarchicalSearch.aspx). Since the 1940s, the chemical constituents of PN have been systematically studied, and the plant has been reported to contain a variety of beneficial ingredients (Krishnamurti and Seshadri, 1946). Pharmacological studies have shown that it has anti-cancer, anti-inflammatory, anti-oxidation, anti-fungal, anti-virus, and other activities. PN as a diuretic is widely used in clinical medicine, as a traditional treatment in Brazil (Kaur et al., 2017; Kieley et al., 2008). In addition, A.H.Campos et al. (Freitas et al., 2002) and J.L.Nishiura et al. (Nishiura et al., 2004) have shown via experimental and clinical studies, respectively, that PN can treat kidney stones.

Urolithiasis or kidney stones is a common and frequently occurring disease worldwide. It is mainly characterized by back pain, abdominal pain, hematuria, nausea, and vomiting. It can cause serious urinary tract infection, acute renal function declines, urinary tract obstruction, and other adverse consequences. The prevalence of urolithiasis in China is 7.54%, and the recurrence rate is 50% 5–10 years after the first treatment (Wang et al., 2017). Stone formation in urolithiasis occurs due to the accumulation of human metabolites, therefore, some patients are closely related to metabolic factors. Metabolic abnormalities, such as hypercalciuria, hyperoxaluria, and hyperuricemia, occur in a high proportion of patients with kidney stones (Abu-Ghanem et al., 2016). Calcium oxalate (CaOx) crystals are implicated in 80% of urolithiasis cases (Evan, 2010; Khan et al., 2016).

Renal tubular epithelial cells are the primary targets of CaOx-induced renal injury. CaOx crystals interact with renal tubular epithelial cells, resulting in cellular injury that becomes the attachment site of crystals (Scheid et al., 2004). The damage of renal tubular epithelial cells leads to further crystallization, crystal retention, and development of stone (Khan, 2004). It is worth noting that during this process, renal tubular cells undergo some adaptive changes to prevent subsequent harm. This reaction is termed acquired renal cytoresistance, which is characterized by the accumulation of cholesterol in cells (Oner and Cirrik, 2009). Cholesterol accumulation increases plasma membrane stability and protects cells from further toxic damage (Zager et al., 1999). However, if left unchecked, these initially beneficial effects may increase the risk of kidney stones (Taguchi et al., 2020; Wang et al., 2022) and progressive renal injury (Kim et al., 2009; Zager et al., 2011). In addition, it is reported that renal tubular cell injury is mediated by lipid accumulation associated with changes in gene expression related to cholesterol transport and synthesis (Kim et al., 2020). In this study, we investigated the mechanisms by which PN manifests its protective effects against CaOx-induced renal injury for a better understanding of its protective properties, especially those related to lipid nephrotoxicity.

2 MATERIALS AND METHODS

2.1 Cell Culture and Treatment

Human renal tubular epithelial HK-2 cells were purchased from American Type Culture Collection (ATCC; Manassas, United States). The cells were cultured in Dulbecco's Modified Eagle Medium/Nutrient Mixture F-12 (DMEM/F-12; Hyclone, United States), containing 10% fetal bovine serum (Gibco, United States), 100 U/mL penicillin, and 100 U/mL streptomycin (Sangon, China). Cells were cultured at 37°C and 5% CO2. The cells were divided into the following three groups: 1) cells in the sodium oxalate (NaOx; Su Yi Chemical Reagent Co., Ltd., Shanghai, China) group were incubated in DMEM/F12 at a concentration of 1 mM (NaOx group) for 12 or 24 h, 2) cells in the Ellagic acid (NaOx + EA

TABLE 1 | List of the 20 active ingredients of *Phyllanthus* niruri L.

No.	Chemical composition	References
1	Quercitrin	Bagalkotkar et al. (2006); Li XR et al. (2007); Kaur et al. (2017); Jantan et al. (2019)
2	Rutin	Bagalkotkar et al. (2006); Li XR et al. (2007); Kaur et al. (2017); Jantan et al. (2019)
3	Niranthin	Bagalkotkar et al. (2006); Li XR et al. (2007); Kaur et al. (2017); Jantan et al. (2019)
4	Nirtetralin	Bagalkotkar et al. (2006); Li XR et al. (2007); Kaur et al. (2017); Jantan et al. (2019)
5	Phyllanthin	Bagalkotkar et al. (2006); Li XR et al. (2007); Kaur et al. (2017); Jantan et al. (2019)
6	Phyltetralin	Bagalkotkar et al. (2006); Li XR et al. (2007); Kaur et al. (2017); Jantan et al. (2019)
7	Corilagin	Bagalkotkar et al. (2006); Li XR et al. (2007); Kaur et al. (2017); Jantan et al. (2019)
8	Ellagic acid	Bagalkotkar et al. (2006); Li XR et al. (2007); Kaur et al. (2017); Jantan et al. (2019)
9	Astragalin	Bagalkotkar et al. (2006); Li XR et al. (2007); Kaur et al. (2017); Jantan et al. (2019)
10	Quercetin	Bagalkotkar et al. (2006); Kaur et al. (2017); Jantan et al. (2019)
11	Lupeol	Bagalkotkar et al. (2006); Kaur et al. (2017); Jantan et al. (2019)
12	Cubebin dimethyl ether	Bagalkotkar et al. (2006); Kaur et al. (2017); Jantan et al. (2019)
13	Urinatetralin	Bagalkotkar et al. (2006); Li XR et al. (2007); Kaur et al. (2017)
14	Hinokinin	Li XR et al. (2007); Kaur et al. (2017); Jantan et al. (2019)
15	Hypophyllanthin	Bagalkotkar et al. (2006); Kaur et al. (2017); Jantan et al. (2019)
16	Isolintetralin	Bagalkotkar et al. (2006); Li XR et al. (2007); Jantan et al. (2019)
17	Lintetralin	Bagalkotkar et al. (2006); Li XR et al. (2007); Kaur et al. (2017)
18	Phyllnirurin	Bagalkotkar et al. (2006); Li XR et al. (2007); Kaur et al. (2017)
19	Phyllanthine	Bagalkotkar et al. (2006); Li XR et al. (2007); Kaur et al. (2017)
20	Gallic acid	Bagalkotkar et al. (2006); Kaur et al. (2017); Jantan et al. (2019)

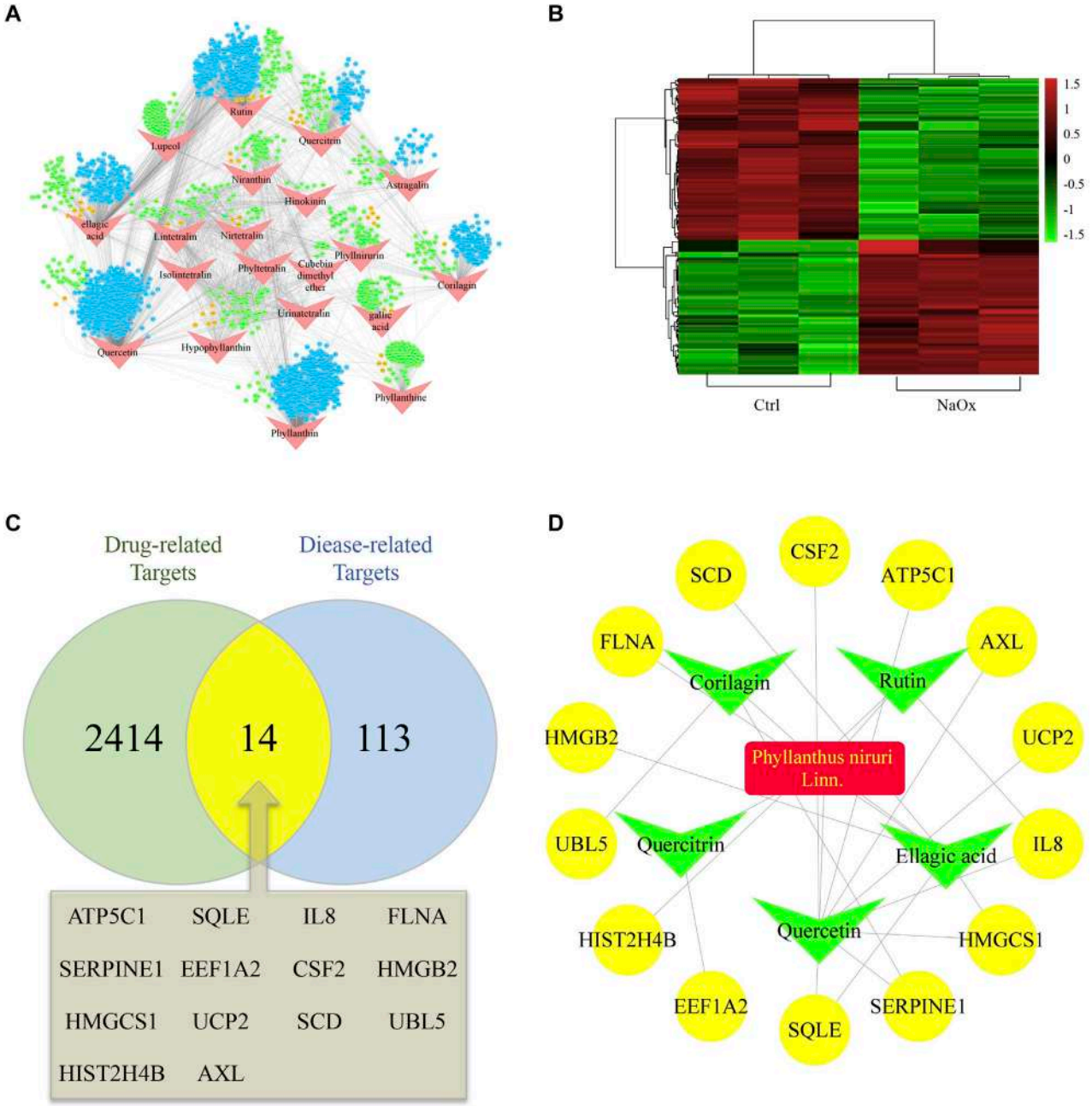

FIGURE 1 | Hub ingredients and targets screening **(A)** An ingredient-target network and nodes represent ingredients (red) and targets form STITCH (blue), Pharmmapper (green) or both (orange) **(B)** Heatmap of potential disease-related targets on microarray analysis between HK-2 cells cultured with (NaOx group) or without (Ctrl group) NaOx **(C)** Venn diagram showing the overlap of diease-related (Oxalate-induced renal injury related) targets (blue) and drug-related (*Phyllanthus* niruri. L related) targets (green) **(D)** The active ingredient-predicted therapeutic target network.

group) were incubated in DMEM/F12 for 12 or 24 h, 3) cells in the PBS were incubated in DMEM/F12 (Ctrl group). The EA concentration was selected based on the results of a Cell Counting Kit 8 (CCK8) assay (Beyotime, China). EA was purchased from Source Leaf Creature (Shanghai, China).

2.2 Microarray Analysis

The duration (24 h) and concentration (1 mM) of NaOx exposure of the cell model were set based on the results of a previous study (Huang et al., 2005). Microarray analysis was performed using Affymetrix HTA 2.0 Transcriptome Arrays.

TABLE 2 | The AutoDock Score of putative targets with ellagic acid and the amino acid residue of targets via hydrogen bonds and hydrophobic contact.

Gene	PDB accession number	Ligand ID	Autodock score (kcal/mol)	Hydrophilic interactions	Hydrophobic contacts
SCD	6C6R	FAD	−10.6	Thr261(A), Trp262(A), Asn148(A)	His157(A), Asn265(A), Val264(A), His171(A), Asp156(A), Trp153(A), Trp184(A), Gln147(A)
SQLE	4ZYO	ST9	−9.8	Asp408(A),Gly420(A), Phe166(A),Glu165(A), Tyr335(A), Ile162(A)	Gly419(A), Gly418(A), Gly164(A), Val163(A), Leu345(A), Pro415(A)
HMGCS1	2P8U	COA	−7.6	Scy129(A), Tyr163(A), Tyr267(A), Ser377(A)	Tyr375(A), Ser221(A), Phe204(A), Val216(A), Ala168(A), Ile222(A), Leu270(A)

2.3 Network Pharmacology

The active ingredients in PN were determined from available data reported in the literature and the potential drug-related targets were determined from the STITCH database (confidence score > 0.15, http://stitch.embl.de/) and PharmMapper Server (The top 100 pharmacophore candidates, http://www.lilab-ecust.cn/pharmmapper/). The disease-related targets were screened from microarray analysis and the conditions were set as FC ≥ 2 and p value < 0.05 or FC ≤ 0.5 and p value < 0.05. Next, the targets of PN active ingredients were mapped to disease-related targets to obtain the predicted therapeutic targets. The active ingredient-target network was constructed using Cytoscape (version 3.8.0) to comprehensively understand the complex interactions between PN, its active ingredients, and their therapeutic targets. The main active ingredients and their putative therapeutic targets were determined.

2.4 Molecular Docking

Molecular docking was performed using AutoDock Vina (version 1.1.2, US) (Trott and Olson, 2010). The simplified molecular input line entry system (SMILES) structure of EA (ingredient CID: 5,281,855) was obtained from PubChem (https://pubchem.ncbi.nlm.nih.gov/). The interactions between EA and its putative therapeutic targets were predicted by AutoDock Vina. The docking scores (to predict binding affinity) and the EA-protein complexes were extracted from AutoDock Vina. Ligand-protein interactions were analyzed using LigPlus (version 2.24, UK) (Laskowski and Swindells, 2011) software and two-dimensional figures were obtained. Then, the PyMoL (version 4.5.0, https://www.schrodinger.com/pymol) is used to make three-dimensional figures.

2.5 Animals

Male C57BL/6 mice aged 6 weeks were (Changzhou Cavens Lab Animal Co., Ltd. Jiangsu, China) maintained in a special pathogen-free (SPF) animal house at 25°C with 12 h of light per day and free access to water and food. All animal procedures are approved by the Laboratory Animal Ethics Committee of Naval Medical University. The mice (n = 18) were randomly divided into the following three groups: control group (Con; n = 6), glyoxylate-induced CaOx group (Gly; n = 6), and EA treatment group (Gly + EA; n = 6). The Gly and Gly + EA group mice were subjected to intraperitoneal injection of glyoxylate (80 mg/kg; UDChem Technology Co., Ltd. Shanghai, China) once daily for 7 days and the Con group was treated with the same volume of saline. The Gly + EA group was intragastrically administrated once daily with EA (20 mg/kg) for 7 days. On the eighth day, all mice were sacrificed; their left kidney tissues were collected and fixed in 10% formaldehyde, embedded in paraffin, cut into 4 μm sections, subjected to hematoxylin and eosin (HE) staining and immunohistochemical analysis; after the right kidney was homogenized, the relative calcium content of total protein, GPx activities, and MDA content were determined by calcium assay kit, GPx, and MDA detection kits, respectively. (Jiancheng, Nanjing, China). The blood was collected and centrifuged to extract the serum for serum creatinine detection.

2.6 Western Blot

Total protein was isolated from HK-2 cells. The HK-2 cell proteins samples were incubated with anti-GAPDH (1:1,000, Proteintech), anti-β-actin (1:1,000, Proteintech), anti-SCD (1:1,000, Proteintech), anti-SQLE (1:1,000, Proteintect), anti-HMGCS1(1:1,000, Proteintech) and anti-p53 (1:1,000, Proteintech) overnight. The secondary antibodies (Licor, United States) were incubated at room temperature for 2 h. The intensity of the immunofluorescent signals was detected using the Odyssey fluorescence imaging system (GENE, United States).

2.7 Histology, Immunohistochemistry (IHC) and Immunofluorescence

Mouse kidneys were fixed in 10% formalin, embedded in paraffin, cut into 4 μm-thick sagittal sections, and stained with HE. Treated HK-2 cells were fixed with 4% paraformaldehyde, permeabilized with 1% Triton X-100, and then blocked with BSA. Both HK-2 cells and kidney tissue sections were incubated overnight with anti-SCD (1:1,000, Proteintech), anti-SQLE (1:1,000, Proteintech), and anti-HMGCS1 (1:1,000, Proteintech) antibodies. The cell nuclei were stained with DAPI after incubating with Alexa Fluor 488 (1:100) for 1 h in the dark. The fluorescence intensity of the HK-2 cells was observed under a confocal microscope. Representative IHC images of kidney sections (200x magnification) were selected and semiquantitative analysis of images using ImageJ software (version 1.6.0, US) are displayed.

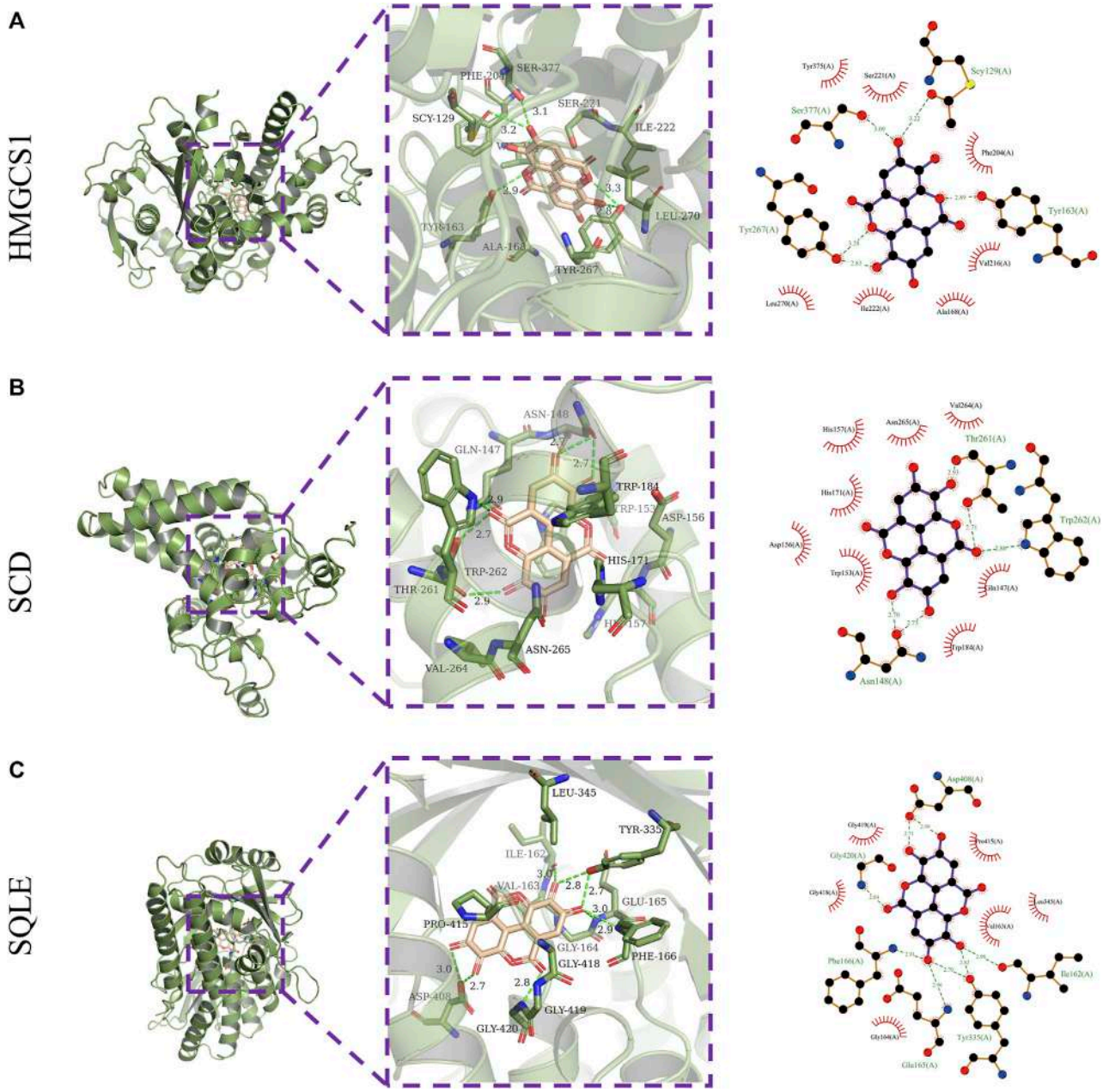

FIGURE 2 | Molecular docking. Three-dimensional (left) and two-dimensional (right) ligand interaction diagrams of ellagic acid and the original ligands of HMGCS1 **(A)**, SCD **(B)**, and SQLE **(C)**.

2.8 Statistical Analysis

The experimental data are expressed as (mean ± standard error). The SPSS (version 19.0, US) software was used for statistical data analysis. Graphs were made using GraphPad Prism (version 9.0, US). The independent *t*-test and one-way ANOVA analysis were used for analyzing the difference between experimental groups. A difference of $p < 0.05$ between the groups was considered statistically significant.

3 RESULTS

3.1 Network Pharmacology Analyses

3.1.1 Active Ingredient Screening

The active ingredients in PN were determined from literature (Bagalkotkar et al., 2006; Li et al., 2007; Kaur et al., 2017; Jantan et al., 2019). The active ingredients that were discussed in at least 75% of the literature were shortlisted for our analysis. As described in **Table 1** active ingredients of PN were considered for our analysis.

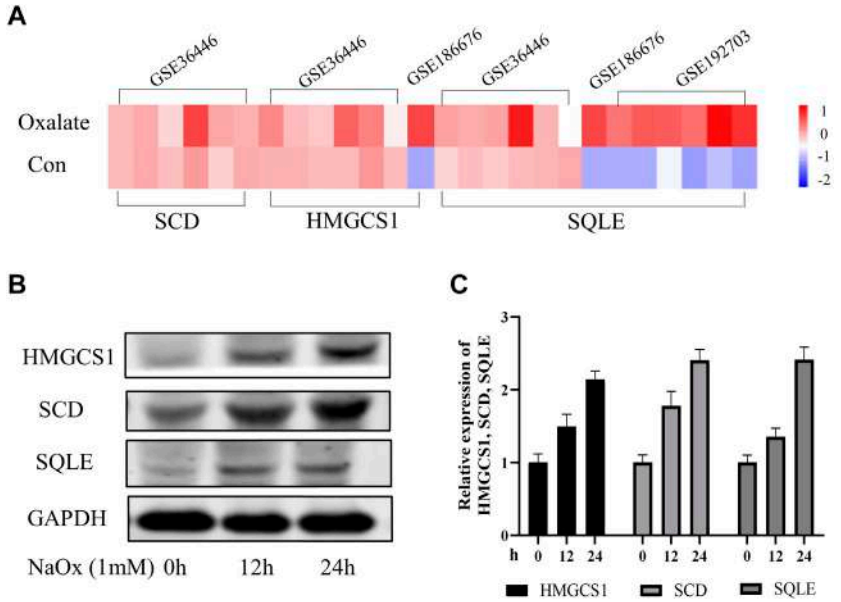

FIGURE 3 | The changing trend of SQLE, HMGCS1, and SCD in oxalate-induced renal injury models **(A)** The Heatmap of SQLE, HMGCS1and SCD were shown in three GSE databases **(B)** Expression of SQLE, HMGCS1 and SCD protein was detected by Western blot in the sodium oxalate group (NaOx) at 0, 12, and 24 h **(C)** Western blot displayed as column charts after quantification.

3.1.2 The Active Ingredient-Predicted Therapeutic Target Network Analysis

The STITCH database and PharmMapper Serve were used together to screen the targets of 20 active ingredients of PN. Totally, 1,688 and 781 potential targets were retrieved from the above two databases, respectively (**Supplementary Tables S1,2**). After removing the repetitive targets, the total amount of obtained potential drug-related targets reduced to 2,428 (**Figure 1A**). In order to probe the potential disease-related targets, we performed transcription profiling on affymetrix microarray HTA 2.0. **Figure Figure1B** shows the differential expression of the 127 targets (**Supplementary Table S3**).

At the intersection of potential drug-related targets and disease-related targets were 14 potential therapeutic targets, as shown by the venn diagram (**Figure 1C**). Inputting this information, an active ingredient-predicted therapeutic target network was visualized using Cytoscape. As shown in **Figures 1A,D** total of 23 relationships (edges) between 20 nodes were identified. Degree of active ingredients analyzed by NetworkAnalyzer tool in Cytoscape (**Supplementary Table S4**), and the top two hub active ingredients, quercetin, and EA were identified. Of interest is that EA has important antioxidant, anti-inflammatory, and anti-apoptotic effects, and has been shown to improve kidney histology and decrease kidney injury biomarker levels (Liu et al., 2020; Neamatallah et al., 2020). In addition, the hub targets corresponding to EA were SQLE, HMGCS1, SCD, HMGB2, and FLNA. Of these, SQLE, HMGCS1, and SCD are related to lipid metabolism and cholesterol synthesis (Brown and Goldstein, 1997; Samuel et al., 2014).

3.1.3 Molecular Modeling and Ligand Docking

Next, the binding affinities between EA and the three therapeutic targets, SQLE, SCD, and HMGCS1, were evaluated using the AutoDock Vina software. Molecular docking programs use scoring functions to evaluate the binding energy of predicting ligand-receptor complexes. As shown in **Table 2**, the scores of the binding energies of EA with SCD, SQLE, and HMGCS1 are −10.6 kcal/mol, −9.8 kcal/mol, and −7.6 kcal/mol, respectively. The two-dimensional and three-dimensional molecular docking diagrams of the three therapeutic targets with EA and its original ligands are shown in **Figure 2** and **Table 2**. All of them have low docked binding energy, which is considered desirable.

3.2 SQLE, HMGCS1 and SCD Expression in the Model of Oxalate Renal Injury

In order to further explore the expression characteristics of SQLE, HMGCS1 and SCD in oxalate renal injury models, we initially screened for potential SQLE, HMGCS1 and SCD by determining transcripts in three data sets (GSE36446, GSE186676, and GSE192703). The GSE datasets were downloaded from the GEO database (https://www.ncbi.nlm.nih.gov/geo/). The results showed that SQLE was up-regulated in mice model of glyoxylate (Gly)-induced oxalate renal injury; SQLE and HMGCS1 were up-regulated in HEK293 T cells model of calcium oxalate monohydrate (COM)-induced oxalate renal injury; SQLE, HMGCS1and SCD were up-regulated in rats model of hydroxy-L-proline (HLP)-induced oxalate renal injury (**Figure 3A**). At the same time, our HK-2 cell model experiment *in vitro* verified that the expressions of SQLE, SCD, and HMGCS1 increased with the increasing time of NaOx stimulation (**Figures 3B,C**, **Supplementary Table S5**). The same trend showed

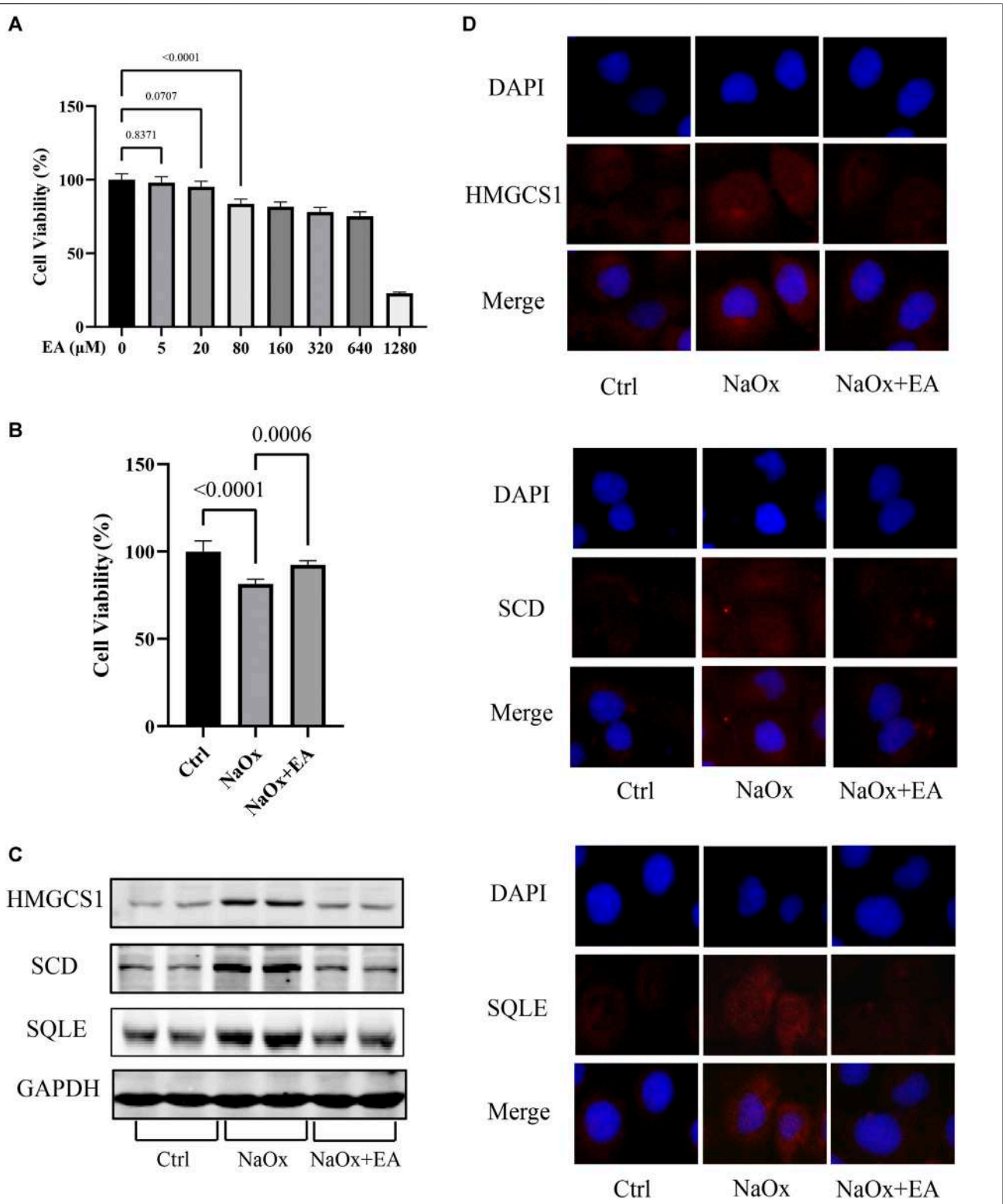

FIGURE 4 | Ellagic acid protects NaOx-induced injury in cells and reduces the expression of SQLE, HMGCS1, and SCD **(A)** The cytotoxicity of ellagic acid on HK-2 cells determined by the CCK8 assay **(B)** The cytotoxicity of ellagic acid on NaOx treated HK-2 cells determined by the CCK8 assay **(C)** The expression of SQLE, HMGCS1, and SCD by Western blot in the control group (Ctrl), sodium oxalate group (NaOx), and ellagic acid treatment group (NaOx + EA) **(D)** Cells were analyzed by immunocytochemistry (100X) in the control group (Ctrl), sodium oxalate group (NaOx), and ellagic acid treatment group (NaOx + EA).

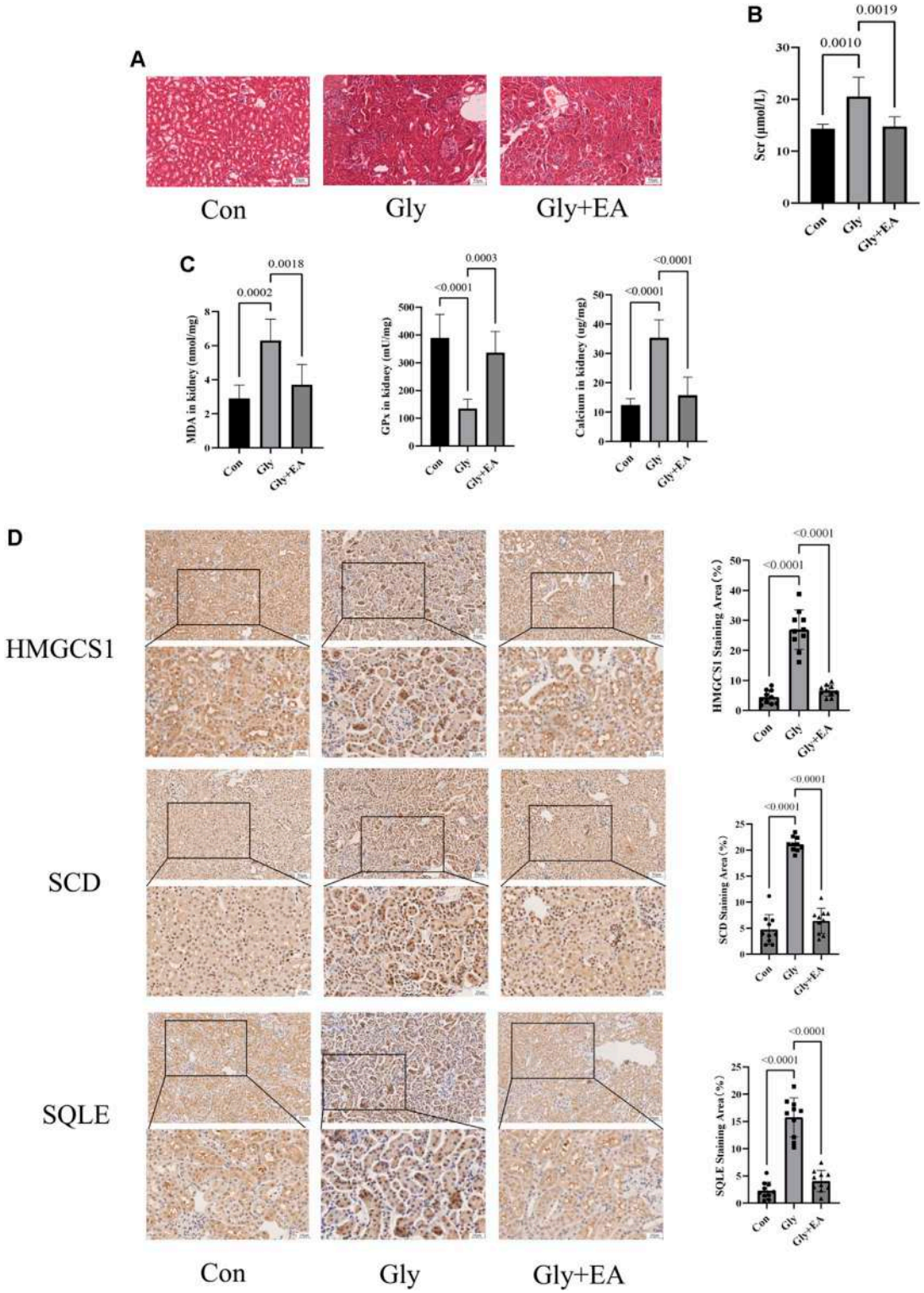

FIGURE 5 | Ellagic acid protects calcium oxalate-induced renal injury in mice and reduces the expression of SQLE, HMGCS1, and SCD **(A)** Representative light microscopy images of hematoxylin and eosin staining of kidneys from the control group (Con), glyoxylate-induced CaOx group (Gly), and ellagic acid treatment group (Gly + EA) (magnification, ×200; scale bar = 50 μm) **(B)** Serum creatinine level in control group (Con), glyoxylate-induced CaOx group (Gly), and ellagic acid treatment group (Gly + EA) **(C)** The GPx activities, MDA, and total calcium content in control group (Con), glyoxylate-induced CaOx group (Gly), and ellagic acid treatment group (Gly + EA) **(D)** Expression of SCD, HMGCS1, and SQLE were analyzed by immunohistochemistry (IHC) (left) Representative light microscopy images of IHC staining of kidney of mice (magnification, ×200; scale bar = 50 μm (up) and 25 μm (down)); (right) Semi-quantitative score of SCD, HMGCS1, and SQLE.

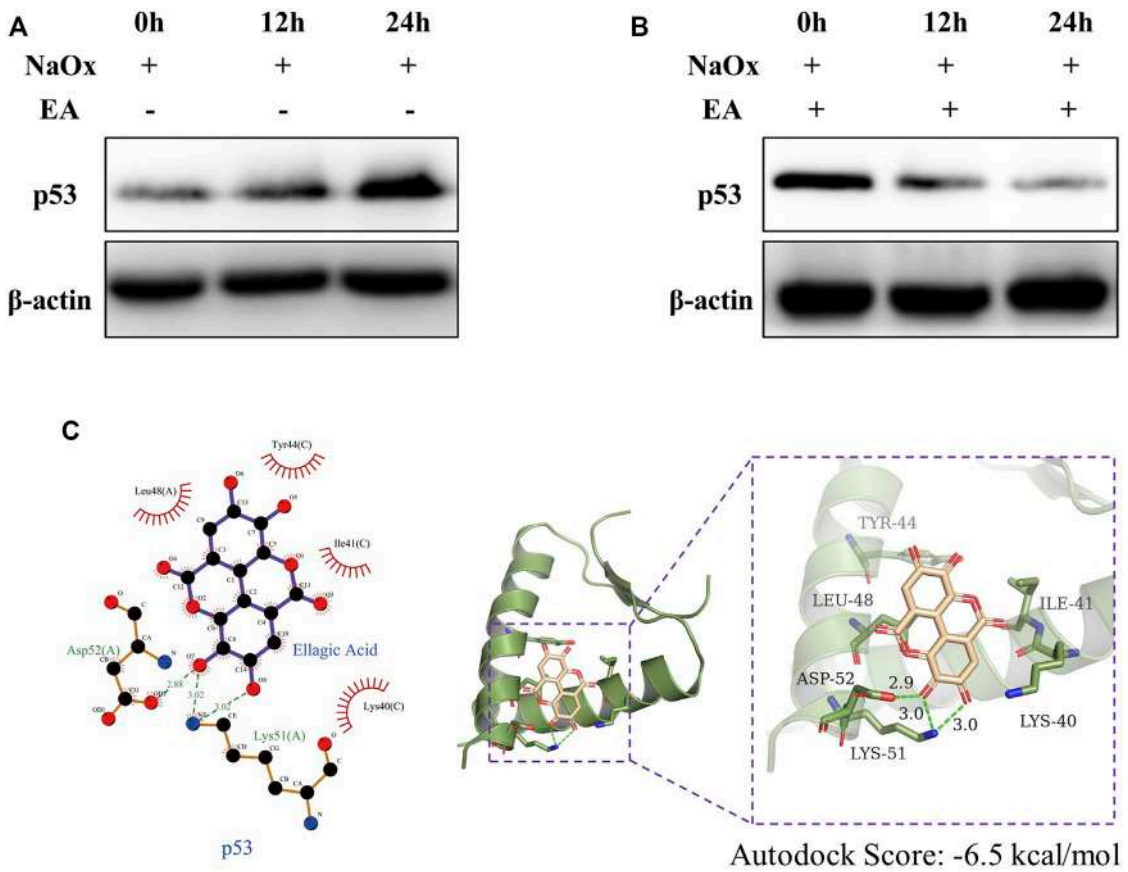

FIGURE 6 | Ellagic acid reduces the expression of p53 **(A)** Expression of p53 protein was detected by western blot in the sodium oxalate group (NaOx) at 0, 12, and 24 h **(B)** Expression of p53 protein was detected by Western blot in the ellagic acid treatment group (NaOx + EA) at 0, 12, and 24 h **(C)** Two-dimensional (left) and three-dimensional (right) ligand interaction diagrams of ellagic acid and the original ligands of p53.

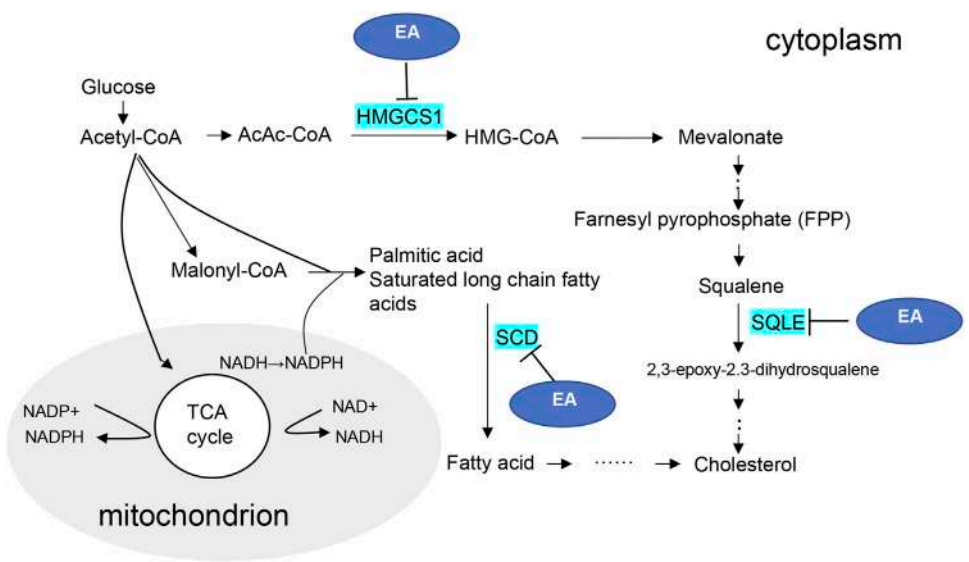

FIGURE 7 | Diagram of the putative regulatory mechanisms of the ellagic acid.

that SCD, HMGCS1 and SQLE were up-regulated in oxalate-induced renal injury.

3.3 Ellagic Acid Protects HK-2 Cells Against Oxalate-Induced Injury by Reducing the Expression of SQLE, HMGCS1, and SCD

The cytotoxic effect of EA was investigated using HK-2 cells with CCK8 assay. As shown in **Figure 4A**, we chose a concentration of 20 μM of EA for the experiments (Supplementary Table S6). Furthermore, The cellular viability of HK-2 cells was inhibited after NaOx stimulation, but restored after treatment with EA (**Figure 4B**, **Supplementary Table S7**). The western blot analysis showed that EA treatment downregulated NaOx-induced injury elevation of SQLE, HMGCS1, and SCD (**Figure 4C**). As shown in **Figure 4D**, the fluorescence intensity of SQLE, HMGCS1, and SCD in the NaOx group was higher than that in the ctrl group, and the fluorescence intensity decreased after EA treatment.

3.4 Ellagic Acid Protects Calcium Oxalate-Induced Renal Injury in Mice by Reducing the Expression of SQLE, HMGCS1, and SCD

As shown in **Figures 5A,B**, EA protects CaOx-induced renal injury in mice. In the HE staining of kidney sections, compared with the Con group, interstitial cell infiltration in Gly mice was significantly more severe. After EA intervention, the injury of renal tubules was gradually alleviated. Serum creatinine level was significantly decreased after EA intervention (**Supplementary Table S8**). In addition, the oxidative stress in mice kidney was evaluated by determining glutathione peroxidase (GPx) activities and malondialdehyde (MDA) content. As shown in **Figure 5C**, MDA content in the Gly mice increased significantly compared with that in the Con mice, and GPx activities in Gly mice decreased significantly compared with those in the Con mice. All changes after EA intervention can be called back. From the total calcium content in the kidney of different groups of mice (**Figure 5C**), it can be seen that EA intervention can significantly reduce the total calcium content of Gly mice. The IHC result was shown in **Figure 5D**, the expression of SCD HMGCS1 and SQLE in the Gly group was considerable increased compared with that in the Con group. After EA treatment, the expression of these indicators decreased. This finding was further confirmed by IHC semiquantitative analysis.

3.5 Ellagic Acid Protects HK-2 Cells Against Oxalate-Induced Injury by Reducing the Expression of p53

We used the PROMO database to predict the common transcription factors of SCD, SQLE, HMGCS1, which also included p53 (**Supplementary Figure S1**). As shown in **Figure 6A**, in our HK-2 cell model experiment *in vitro*, the western blot analysis showed that the expressions of p53 increased with the increasing time of NaOx stimulation. The change can be reversed by the addition of EA (**Figure 6B**). In addition, the results of molecular docking show that the two-dimensional and three-dimensional molecular docking diagrams of p53 with EA (**Figure 6C**). The score of the binding energies is -6.5 kcal/mol.

4 DISCUSSION

Natural herbal medicines are typical multi-component, multitarget, and multi-pathway agents; they contain active ingredients which are responsible for their pharmacological activity. Our study aimed to identify the key active ingredients of PN, which has several medicinal properties, and their putative therapeutic targets based on network pharmacology.

Network pharmacology is a promising approach for the study of traditional Chinese medicine (TCM). In recent years, with the popularization of network pharmacology, an integrated approach of network pharmacology and multi-omics has become an important tool for analyzing the mechanisms of action of TCM. Transcriptomics has been widely applied with network pharmacology analysis to characterize the molecular mechanisms underlying therapeutic effects. In this study, we employed network pharmacology and transcriptomics to analyze the mechanism of PN in the treatment of CaOx-induced renal injury and enabled the identification of the active ingredient (EA) in PN and its core targets (HMGCS1, SQLE, and SCD). Moreover, the experimental results were consistent with the results of network pharmacology mining, increasing the reliability of network pharmacology network prediction.

3-hydroxy-3-methylglutaryl-CoA synthase 1 (HMGCS1) is a metabolic enzyme involved in the formation of 3-hydroxy-3-methylglutaryl-CoA (HMG-CoA), an important substrate in mevalonate pathway (Gruenbacher and Thurnher, 2015). The mevalonate pathway is an enzymatic cascade responsible for synthesizing cholesterol (Thurnher et al., 2013). Squalene epoxidase (SQLE) is one of the rate-limiting enzymes in the biosynthesis of cholesterol. SQLE can further affect the synthesis of cholesterol in mevalonate pathway by affecting the catalysis of squalene (Yu et al., 2020). Stearoyl-CoA desaturase (SCD) is an important regulatory enzyme of *de novo* lipogenesis, which catalyzes the biosynthesis of unsaturated fatty acids (Dobrzyn and Ntambi, 2004). Lipid has two-sided. An appropriate increase can produce a protective effect and an excessive increase can cause oxidative damage, lead to tissue lipid peroxidation, and finally cause lipotoxicity. Lipid homeostasis is crucial to prevent lipotoxicity. Our *in vivo* and *in vitro* experiments showed that SQLE, SCD and HMGCS1 increased significantly in the CaOx-induced renal injury models, suggesting the existence of lipid nephrotoxicity and progressive renal injury.

In addition, more and more evidence supports the lipid metabolism mediated by p53 tumor suppressor. The studies of Lacroix M et al. (Lacroix et al., 2021) suggest the importance of p53-SCD axis in lipid metabolism. The effect of p53 on Mevalonate Pathway was also suggested in the study of Freed-Pastor WA et al.

(Freed-Pastor et al., 2012). The results of molecular docking not only suggested that EA might interact with SCD, SQLE, HMGCS1 protein directly, but also suggested that p53 transcription factor might regulate the above three targets. The results of immunoblotting imply the regulatory effect. Therefore, we speculate that EA may not only directly bind to SCD, SQLE, HMGCS1 and inhibit its expression, but also indirectly affect p53 and further affect the three downstream proteins.

In CaOx-induce renal injury, crystals precipitate in renal tubules and interact with renal tubular epithelial cells to induce oxidative stress and inflammation (Khan et al., 2021). Excessive oxidative stress and inflammation will not only increase the deposition and retention of oxalate crystals in tubular cells, but also lead to the development of fibrosis (Khan, 2014). Epithelial mesenchymal transition (EMT) is an important initial link of renal interstitial fibrosis and plays an important role in the repair of renal tissue injury (Kalluri and Neilson, 2003). In renal crystal induced renal injury, EMT occurs in renal tubular epithelial cells in the early stage of renal stone formation or crystal induced renal injury, and then triggers the process of renal fibrosis (Hu et al., 2015). Sun Y et al. (Sun et al., 2020) confirmed that the increase of renal cholesterol caused by abnormal cholesterol metabolism will increase oxidative stress injury. Kong YL et al. (Kong et al., 2020) confirmed that the excessive accumulation of cholesterol in cells may stimulate the increase of NLRP3 and induce inflammatory response. In addition, Accumulation of cholesterol can activate PI3K-Akt signaling pathway (Yue et al., 2014). Activated PI3K-Akt signaling pathway will aggravate renal inflammation and oxidative stress injury (Ang et al., 2015). Si YC et al. (Si et al., 2021) confirmed that inhibiting the activation of PI3K-Akt signaling pathway in oxalate crystallization mouse model can reduce crystalline kidney injury and inhibit the occurrence and development of EMT. In conclusion, we can speculate that abnormal cholesterol metabolism leads to the accumulation of cholesterol, which may increase the damage of oxidative stress, inflammation and fibrosis in the kidney.

EA is an active natural polyphenol ingredient with antibacterial, anti-inflammatory, hepatoprotective, anti-obesity, and anti-tumor effects (Chen et al., 2018). Furthermore, several studies have shown that EA can modulate lipid metabolism, which inhibits lipid accumulation by suppressing early adipogenic events and cell cycle arrest (Okla et al., 2015; Woo et al., 2015). Therefore, synthesize our experimental verification results, the possible mechanism diagram of EA regulating lipid metabolism in CaOx-induced renal injury was shown in **Figure 7**. Considering the molecular docking results, we speculate that EA may reduce the transformation of cholesterol in damaged HK-2 cells and protect cells in CaOx-induced renal injury by inhibiting the activities of HMGCS1, SCD, and SQLE.

DATA AVAILABILITY STATEMENT

The datasets presented in this study can be found in online repositories. The names of the repository/repositories and accession number(s) can be found in the article/**Supplementary Material**.

ETHICS STATEMENT

The animal study was reviewed and approved by Committee on Ethic of Medical Research, Naval Medical University (registration number: NMUMREC-2021-006).

AUTHOR CONTRIBUTIONS

Conceptualization, Z-YG and WC; methodology, M-TL, L-LL, and L-XH; formal analysis, M-TL, QZ, and Y-XS; investigation, M-TL, L-LL, QZ, and J-BH; resources, L-LL, QZ, and H-TL; writing—original draft preparation, M-TL, L-LL, and QZ; writing—review and editing, Z-YG and WC; visualization, BY; supervision, Z-YG and WC; funding acquisition, Z-YG, BY, and J-BH. All authors have read and agreed to the published version of the manuscript.

FUNDING

This research was funded by National Key R&D Program of China (2018YFA0107500), National Natural Science Foundation of China (Nos. 81903962,82070692,82173369) and "234" subject peak climbing plan of Changhai Hospital (2019YXK043).

SUPPLEMENTARY MATERIAL

The Supplementary Material for this article can be found online at: https://www.frontiersin.org/articles/10.3389/fphar.2022.891788/full#supplementary-material

REFERENCES

Abu-Ghanem, Y., Kleinmann, N., Winkler, H. Z., and Zilberman, D. E. (2016). Nephrolithiasis in Israel: Epidemiological Characteristics of Return Patients in a Tertiary Care Center. *Isr. Med. Assoc. J.* 18, 725–728.

Ang, L., Yuguang, L., Liying, W., Shuying, Z., Liting, X., and Shumin, W. (2015). Ergosterol Alleviates Kidney Injury in Streptozotocin-Induced Diabetic Mice. *Evid. Based Complement. Altern. Med.* 2015, 691594. doi:10.1155/2015/691594

Bagalkotkar, G., Sagineedu, S. R., Saad, M. S., and Stanslas, J. (2006). Phytochemicals from Phyllanthus Niruri Linn. And Their Pharmacological Properties: a Review. *J. Pharm. Pharmacol.* 58, 1559–1570. doi:10.1211/jpp.58.12.0001

Brown, M. S., and Goldstein, J. L. (1997). The SREBP Pathway: Regulation of Cholesterol Metabolism by Proteolysis of a Membrane-Bound Transcription Factor. *Cell.* 89, 331–340. doi:10.1016/s0092-8674(00)80213-5

Chen, P., Chen, F., and Zhou, B. (2018). Antioxidative, Anti-inflammatory and Anti-apoptotic Effects of Ellagic Acid in Liver and Brain of Rats Treated by D-Galactose. *Sci. Rep.* 8, 1465. doi:10.1038/s41598-018-19732-0

Dobrzyn, A., and Ntambi, J. M. (2004). The Role of Stearoyl-CoA Desaturase in Body Weight Regulation. *Trends Cardiovasc Med.* 14, 77–81. doi:10.1016/j.tcm.2003.12.005

Evan, A. P. (2010). Physiopathology and Etiology of Stone Formation in the Kidney and the Urinary Tract. *Pediatr. Nephrol.* 25, 831–841. doi:10.1007/s00467-009-1116-y

Freed-Pastor, W. A., Mizuno, H., Zhao, X., Langerød, A., Moon, S. H., Rodriguez-Barrueco, R., et al. (2012). Mutant P53 Disrupts Mammary Tissue Architecture via the Mevalonate Pathway. *Cell.* 148 (1-2), 244–258. doi:10.1016/j.cell.2011.12.017

Freitas, A. M., Schor, N., and Boim, M. A. (2002). The Effect of Phyllanthus Niruri on Urinary Inhibitors of Calcium Oxalate Crystallization and Other Factors Associated with Renal Stone Formation. *BJU Int.* 89, 829–834. doi:10.1046/j.1464-410x.2002.02794.x

Gruenbacher, G., and Thurnher, M. (2015). Mevalonate Metabolism in Cancer. *Cancer Lett.* 356, 192–196. doi:10.1016/j.canlet.2014.01.013

Hu, H., Chen, W., Ding, J., Jia, M., Yin, J., and Guo, Z. (2015). Fasudil Prevents Calcium Oxalate Crystal Deposit and Renal Fibrogenesis in Glyoxylate-Induced Nephrolithic Mice. *Exp. Mol. Pathol.* 98 (2), 277–285. doi:10.1016/j.yexmp.2015.02.006

Huang, M. Y., Chaturvedi, L. S., Koul, S., and Koul, H. K. (2005). Oxalate Stimulates IL-6 Production in HK-2 Cells, a Line of Human Renal Proximal Tubular Epithelial Cells. *Kidney Int.* 68, 497–503. doi:10.1111/j.1523-1755.2005.00427.x

Jantan, I., Haque, M. A., Ilangkovan, M., and Arshad, L. (2019). An Insight into the Modulatory Effects and Mechanisms of Action of Phyllanthus Species and Their Bioactive Metabolites on the Immune System. *Front. Pharmacol.* 10, 878. doi:10.3389/fphar.2019.00878

Kalluri, R., and Neilson, E. G. (2003). Epithelial-mesenchymal Transition and its Implications for Fibrosis. *J. Clin. Investig.* 112 (12), 1776–1784. doi:10.1172/JCI20530

Kaur, N., Kaur, B., and Sirhindi, G. (2017). Phytochemistry and Pharmacology of Phyllanthus Niruri L.: A Review. *Phytother. Res.* 31, 980–1004. doi:10.1002/ptr.5825

Khan, S. R., Canales, B. K., and Dominguez-Gutierrez, P. R. (2021). Randall's Plaque and Calcium Oxalate Stone Formation: Role for Immunity and Inflammation. *Nat. Rev. Nephrol.* 17 (6), 417–433. doi:10.1038/s41581-020-00392-1

Khan, S. R., Pearle, M. S., Robertson, W. G., Gambaro, G., Canales, B. K., Doizi, S., et al. (2016). Kidney Stones. *Nat. Rev. Dis. Prim.* 2, 16008. doi:10.1038/nrdp.2016.8

Khan, S. R. (2004). Role of Renal Epithelial Cells in the Initiation of Calcium Oxalate Stones. *Nephron Exp. Nephrol.* 98, e55–60. doi:10.1159/000080257

Khan, S. R. (2014). Reactive Oxygen Species, Inflammation and Calcium Oxalate Nephrolithiasis. *Transl. Androl. Urol.* 3 (3), 256–276. doi:10.3978/j.issn.2223-4683.2014.06.04

Kieley, S., Dwivedi, R., and Monga, M. (2008). Ayurvedic Medicine and Renal Calculi. *J. Endourol.* 22, 1613–1616. doi:10.1089/end.2008.0020

Kim, H. J., Moradi, H., Yuan, J., Norris, K., and Vaziri, N. D. (2009). Renal Mass Reduction Results in Accumulation of Lipids and Dysregulation of Lipid Regulatory Proteins in the Remnant Kidney. *Am. J. Physiol. Ren. Physiol.* 296, F1297–F1306. doi:10.1152/ajprenal.90761.2008

Kim, Y. J., Oh, S. H., Ahn, J. S., Yook, J. M., Kim, C. D., Park, S. H., et al. (2020). The Crucial Role of Xanthine Oxidase in CKD Progression Associated with Hypercholesterolemia. *Int. J. Mol. Sci.* 21, 7444. doi:10.3390/ijms21207444

Kong, Y., Feng, W., Zhao, X., Zhang, P., Li, S., Li, Z., et al. (2020). Statins Ameliorate Cholesterol-Induced Inflammation and Improve AQP2 Expression by Inhibiting NLRP3 Activation in the Kidney. *Theranostics* 10 (23), 10415–10433. doi:10.7150/thno.49603

Krishnamurti, G. V., and Seshadri, T. R. (1946). The Bitter Principle ofPhyllanthus Niruri. *Proc. Indian Acad. Sci. Math. Sci.)* 24, 357. doi:10.1007/BF03171072

Lacroix, M., Linares, L. K., Rueda-Rincon, N., Bloch, K., Di Michele, M., De Blasio, C., et al. (2021). The Multifunctional Protein E4F1 Links P53 to Lipid Metabolism in Adipocytes. *Nat. Commun.* 12 (1), 7037. doi:10.1038/s41467-021-27307-3

Laskowski, R. A., and Swindells, M. B. (2011). LigPlot+: Multiple Ligand-Protein Interaction Diagrams for Drug Discovery. *J. Chem. Inf. Model.* 51, 2778–2786. doi:10.1021/ci200227u

Li, X. R., Zhou, W., and Wei, W. X. (2007). Chemical Components and Bioactivities of Phyllanthus Niruri L. *Nat. Prod. Res. Dev.* 19, 890. doi:10.16333/j.1001-6880.2007.05.040

Liu, Q., Liang, X., Liang, M., Qin, R., Qin, F., and Wang, X. (2020). Ellagic Acid Ameliorates Renal Ischemic-Reperfusion Injury through NOX4/JAK/STAT Signaling Pathway. *Inflammation* 43, 298–309. doi:10.1007/s10753-019-01120-z

Neamatallah, T., El-Shitany, N., Abbas, A., Eid, B. G., Harakeh, S., Ali, S., et al. (2020). Nano Ellagic Acid Counteracts Cisplatin-Induced Upregulation in OAT1 and OAT3: A Possible Nephroprotection Mechanism. *Molecules*. 25: 3031 doi:10.3390/molecules25133031

Nishiura, J. L., Campos, A. H., Boim, M. A., Heilberg, I. P., and Schor, N. (2004). Phyllanthus Niruri Normalizes Elevated Urinary Calcium Levels in Calcium Stone Forming (CSF) Patients. *Urol. Res.* 32, 362–366. doi:10.1007/s00240-004-0432-8

Okla, M., Kang, I., Kim, D. M., Gourineni, V., Shay, N., Gu, L., et al. (2015). Ellagic Acid Modulates Lipid Accumulation in Primary Human Adipocytes and Human Hepatoma Huh7 Cells via Discrete Mechanisms. *J. Nutr. Biochem.* 26, 82–90. doi:10.1016/j.jnutbio.2014.09.010

Oner, G., and Cirrik, S. (2009). The Nephrotoxicity Risk in Rats Subjected to Heavy Muscle Activity. *J. Sports Sci. Med.* 8, 481–488.

Samuel, W., Kutty, R. K., Duncan, T., Vijayasarathy, C., Kuo, B. C., Chapa, K. M., et al. (2014). Fenretinide Induces Ubiquitin-dependent Proteasomal Degradation of Stearoyl-CoA Desaturase in Human Retinal Pigment Epithelial Cells. *J. Cell. Physiol.* 229, 1028–1038. doi:10.1002/jcp.24527

Scheid, C. R., Cao, L. C., Honeyman, T., and Jonassen, J. A. (2004). How Elevated Oxalate Can Promote Kidney Stone Disease: Changes at the Surface and in the Cytosol of Renal Cells that Promote Crystal Adherence and Growth. *Front. Biosci.* 9, 797–808. doi:10.2741/1265

Si, Y., Liu, L., Cheng, J., Zhao, T., Zhou, Q., Yu, J., et al. (2021). Oral Hydrogen-Rich Water Alleviates Oxalate-Induced Kidney Injury by Suppressing Oxidative Stress, Inflammation, and Fibrosis. *Front. Med.* 8, 713536. doi:10.3389/fmed.2021.713536

Sun, Y., Ge, X., Li, X., He, J., Wei, X., Du, J., et al. (2020). High-fat Diet Promotes Renal Injury by Inducing Oxidative Stress and Mitochondrial Dysfunction. *Cell. Death Dis.* 11 (10), 914. doi:10.1038/s41419-020-03122-4

Taguchi, K., Chen, L., Usawachintachit, M., Hamamoto, S., Kang, M., Sugino, T., et al. (2020). Fatty Acid-Binding Protein 4 Downregulation Drives Calcification in the Development of Kidney Stone Disease. *Kidney Int.* 97, 1042–1056. doi:10.1016/j.kint.2020.01.042

Thurnher, M., Gruenbacher, G., and Nussbaumer, O. (2013). Regulation of Mevalonate Metabolism in Cancer and Immune Cells. *Biochim. Biophys. Acta* 1831, 1009–1015. doi:10.1016/j.bbalip.2013.03.003

Trott, O., and Olson, A. J. (2010). AutoDock Vina: Improving the Speed and Accuracy of Docking with a New Scoring Function, Efficient Optimization, and Multithreading. *J. Comput. Chem.* 31, 455–461. doi:10.1002/jcc.21334

Wang, B., Wei, J., Huangfu, Q., Gao, F., Qin, L., Zhong, J., et al. (2022). Identification of Resolvin D1 and Protectin D1 as Potential Therapeutic Agents for Treating Kidney Stones. *Oxid. Med. Cell Longev.* 2022, 4345037. doi:10.1155/2022/4345037

Wang, W., Fan, J., Huang, G., Li, J., Zhu, X., Tian, Y., et al. (2017). Prevalence of Kidney Stones in Mainland China: A Systematic Review. *Sci. Rep.* 7, 41630. doi:10.1038/srep41630

Woo, M. S., Choi, H. S., Seo, M. J., Jeon, H. J., and Lee, B. Y. (2015). Ellagic Acid Suppresses Lipid Accumulation by Suppressing Early Adipogenic Events and Cell Cycle Arrest. *Phytother. Res.* 29, 398–406. doi:10.1002/ptr.5264

Yu, Z., He, Q., and Xu, G. (2020). Screening of Prognostic Factors in Early-Onset Breast Cancer. *Technol. Cancer Res. Treat.* 19, 1533033819893670. doi:10.1177/1533033819893670

Yue, S., Li, J., Lee, S. Y., Lee, H. J., Shao, T., Song, B., et al. (2014). Cholesteryl Ester Accumulation Induced by PTEN Loss and PI3K/AKT Activation Underlies Human Prostate Cancer Aggressiveness. *Cell. Metab.* 19, 393–406. doi:10.1016/j.cmet.2014.01.019

Zager, R. A., Burkhart, K. M., Johnson, A. C., and Sacks, B. M. (1999). Increased Proximal Tubular Cholesterol Content: Implications for Cell Injury and "acquired Cytoresistance". *Kidney Int.* 56, 1788–1797. doi:10.1046/j.1523-1755.1999.00745.x

Zager, R. A., Johnson, A. C., and Becker, K. (2011). Acute Unilateral Ischemic Renal Injury Induces Progressive Renal Inflammation, Lipid Accumulation,

Histone Modification, and "End-Stage" Kidney Disease. *Am. J. Physiol. Ren. Physiol.* 301, F1334–F1345. doi:10.1152/ajprenal.00431.2011

Conflict of Interest: The authors declare that the research was conducted in the absence of any commercial or financial relationships that could be construed as a potential conflict of interest.

Publisher's Note: All claims expressed in this article are solely those of the authors and do not necessarily represent those of their affiliated organizations, or those of the publisher, the editors and the reviewers. Any product that may be evaluated in this article, or claim that may be made by its manufacturer, is not guaranteed or endorsed by the publisher.

The Renal Protective Potential Effect of Infusion of Anti-urolithiasis Formula in Urolithiasis Patients: A Randomized Clinical Study

Ulfatun Nisa[1][a], Peristiwan Ridha Widhi Astana[1][b], Saryanto[1][c], Tyas Friska Dewi[1][d] and Enggar Wijayanti[1][e]

[1]*Medicinal Plant and Traditional Medicine Research and Development Center, Ministry of Health, Tawangmangu, Indonesia*

Keywords: Renoprotective, Anti–urolithiasis Formula, Urolithiasis Disease

Abstract: Kidney stones and related urological procedures can lead to chronic kidney disease (CKD). The constituent plants of an anti-urolithiasis formula developed by B2P2TOOT have a potential renoprotective effect, thus preventing CKD progression. This randomized open-label clinical study with end-blinded observation was aimed to evaluate the possible renoprotective effect of anti-urolithiasis formula infusions in urolithiasis patients. Two hundred volunteer subjects were randomly allocated into two groups: anti-urolithiasis herbal formula (AHF) and commercial polyextract lithotripsy (CPL). Urine tests were performed, and the estimated glomerular filtration rate (eGFR) was calculated using a CKD-EPI equation at baseline (day 0) and after the intervention (day 56). The analysis was done within each group and between both groups using paired sample T-test and independent T-tests. An increase in the eGFR of subjects in the AHF group was found, although it was not statistically significant (p=0.35). The mean of the eGFR of subjects in the CPL group after the intervention was lower, also statistically insignificant (p=0.56). Nevertheless, there were significant differences in the eGFR after intervention between both groups (p=0.044, 95% CI 0.16–12.4). Our findings suggest that AHF has a slight potential effect on renal function preservation in urolithiasis patients.

1 INTRODUCTION

Urolithiasis has become a worldwide health burden. Its incidence rates are 10% for men and 5% for women (D'Costa *et al*., 2016). The high recurrence rate of urolithiasis results in health financing issues and considerable morbidity (Lee *et al*., 2015). Also, several studies have revealed that the formation of stones in the urinary tract has a strong correlation with adverse renal outcomes. However, the mechanism underlying kidney stones and diminished kidney function is likely multifactorial (Alexander *et al*., 2012; Coe *et al*., 2010). Urolithiasis plays a significant role in influencing the risk of adverse renal outcomes and prior history of recurrent symptomatic episodes. Accordingly, it might produce an increased risk of end-stage renal disease (ESRD). For example, the progressive calcification of calcium kidney stones at the tubular basement membrane and the ducts of Bellini causes renal damage through progressive scarring, leading to ESRD (Coe *et al*., 2010; Evan, 2010).

Urolithiasis management has recently played an essential role in preventing several future health complications—one of the standard procedures in the management of nephrolithiasis is extracorporeal shock wave lithotripsy (ESWL). ESWL had been regularly utilized in the management of urolithiasis. Nevertheless, it might significantly contribute to the increased risk of recurring stones and result in greater difficulty when comminuting stones with ESWL (Evan, 2010). Moreover, it can result in several complications, leading to kidney function loss (Shekar Kumaran and Patki, 2011). This hypothesis

[a] https://orcid.org/0000-0001-8743-3121
[b] https://orcid.org/0000-0002-7341-4330
[c] https://orcid.org/0000-0002-0442-8261
[d] https://orcid.org/0000-0002-4467-9372
[e] https://orcid.org/0000-0002-1322-6784

Nisa, U., Widhi Astana, P., Saryanto, ., Dewi, T. and Wijayanti, E.
The Renal Protective Potential Effect of Infusion of Anti-urolithiasis Formula in Urolithiasis Patients: A Randomized Clinical Study.
DOI: 10.5220/0010488300910097
In *Proceedings of the 1st Jenderal Soedirman International Medical Conference in conjunction with the 5th Annual Scientific Meeting (Temilnas) Consortium of Biomedical Science Indonesia (JIMC 2020)*, pages 91-97
ISBN: 978-989-758-499-2

has suggested a decrease in renal function by vasoconstriction, and its persistent stone fragments may induce acute renal injury (Agawane *et al*., 2019; Khan *et al*., 2011; Nizami *et al*., 2012; Srisubat *et al*., 2014). By contrast, another study found no correlation between ESWL and CKD development (D'Costa *et al*., 2016; E. *et al*., 2008). The retrospective study revealed that urological procedures could significantly increase the risk of developing elevated serum creatinin but were not significant in progressing CKD itself (D'Costa *et al*., 2016). There is no appropriate drug for the treatment of urolithiasis despite technological advances in the field of medicine. However, it is worthwhile to explore the potential benefits of medicinal plants, which may affect anti-urolithiasis and restore renal impairments.

Polyherbal treatment can be considered an alternative approach to treating urolithiasis. The investigation of phytotherapy for urolithiasis has been reported in an ethnopharmacology study, in vitro, and in vivo models (Ahmed *et al*., 2016; Akanae *et al*., 2010; Nisa and Astana, 2018; Patankar *et al*., 2020; Yadav, RD., Jain, SK., Alok, Shashi., Mahor, Alok., Bharti, JP., Jaiswal *et al*., 2011). The diuretic activity of *Orthosiphon stamineus* is different when combined with hydrochlorothiazide and furosemide (Adam *et al*., 2009). It takes a longer time to produce effects than synthetic diuretics but, notably, does not include any side effects (Tiwari *et al*., 2017). Meanwhile, *Phyllanthus niruri* can inhibit lithiasis' growth in rats (Morán *et al*., 2013). The administration of *Phyllanthus niruri* can decrease mRNA p65NF-κB and mRNA IL-6 levels in the kidneys of diabetic rats (Giribabu *et al*., 2017). Jonnel B.P. et al. revealed that an increase in *Imperata cylindraca* extract concentration is related to decreased serum creatinine and blood urea nitrogen (BUN) levels. Thus, several medicinal plants appear to have distinct mechanisms for urolithiasis that generate synergetic effects to facilitate stones' passage.

The constituent plants of the anti-urolithiasis formula developed by the Medicinal Plant and Traditional Medicine Research and Development Center (B2P2TOOT-in Bahasa) have a potential renoprotective effect, which suggests they can serve as an alternative method of preventing CKD progression. This method's safety and efficacy have been proven in clinical trials (Nisa and Astana, 2019). Several compositions of the AHF had been reported to have a potential renoprotective effect in a single-use form. This study aims to evaluate the possible renoprotective effect of an anti-urolithiasis herbal formula in urolithiasis patients.

2 MATERIALS AND METHODS

The study was conducted by the Traditional Plant and Traditional Medicine Research and Development Center at the Ministry of Health Indonesian and involved191 urolithiasis patients. The design of the study was a purposive randomized open-label study design, with end-blinded observation. We involved 70 physicians, who all have Saintifikasi Jamu (SJ) certifications as investigators. The ethics committee approved the study protocol of the National Institute of Research and Development (LB.02.01/5.2/KE 063/2016) on March 13th, 2017. The principal investigator was qualified in traditional and allopathic medicine and clinical trials, in accordance with Good Clinical Practices (GCP).

Volunteer patients who fulfilled the inclusion criteria participated in this study. Before participating in the study, each subject was requested to read and sign an informed consent form. The inclusion criteria were: an age of 17-60 years old, a history of urolithiasis, the presence of a stone<2 cm in diameter, serum creatinine levels of<2 g/dl, and liver and kidney function within a normal range. Patients with complications from severe diseases and those requiring surgical intervention were excluded from the study. Eligible subjects were randomized by computer software into two groups: the AHF and the CPL group.

In the AHF group, each subject was given an herbal formula, which consisted of a dried simplisia of 10 g of S. *arvensis*, 6 g of *O. stamineus*, 4 g of *Strobilanthes crispus*, 5 g of *Imperata cylindrica*, 5 g of *C. xanthorrhiza*, 4 g of *Curcuma domestica*, and 3 g of *P. niruri*. Each subject was requested to prepare an infusion from the formula. The AHFwas prepared by boiling 1 L of water, adding the simplisia into the boiling water, and letting the mixture boil for 15 minutes. Subjects were instructed to drink the filtered water twice a day for 56 days, after breakfast and dinner. Meanwhile, in the CPL group, subjects consumed CPL, which consisted of an extract of 18 mg of *O. stamineus*, 6 mg of *S. crispa,* 24 mg of *S. arvensis L*., 2.4 mg of *P. niruri*, and 100 mg of *Plantago major*. They took one capsule of CPL four times daily, also for 56 days.

Demographic data such as age, sex, BMI, history of stone recurrence, and stone size were recorded at day 0 of the study. Urine tests (routine and microscopic), including tests of urine turbidity, pH, specific gravity, LE, Nitrit, RBC, and albuminuria, were performed on days 0, 28, and 56 to observe the fluctuation of urine quality. The kidney's biochemical parameters (creatinine and BUN) were measured on

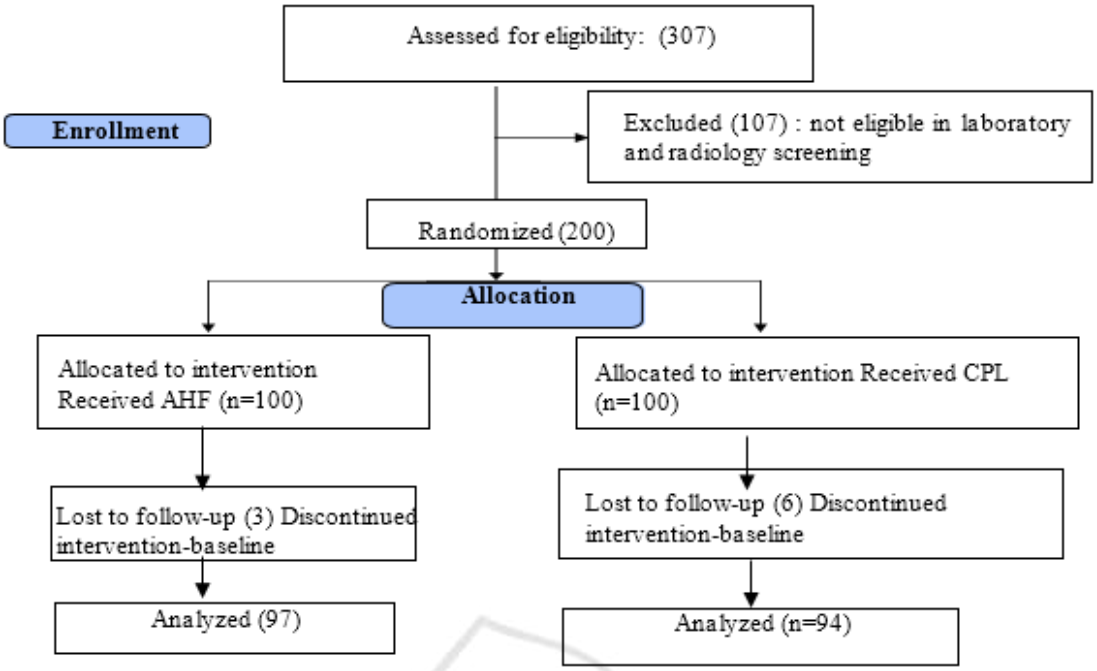

Figure 1: Enrollment, randomization, allocation, follow-up, and analysis

day 0 and day 56, followed by a calculation of the estimated glomerular filtration rate (eGFR) using a CKD-EPI equation.

The data were analyzed statistically using a GraphPad Prism program for statistical analysis version 8.0. Descriptive data were calculated and presented in Table 1. To determine differences before and after treatment, we performed a paired T-test. An independent T-test was also conducted to determine the differences between the two groups. Alternatively, the Wilcoxon test and Mann–Whitney U-test were used when there was an abnormal data distribution in the Kolmogorov–Smirnov test results.

3 RESULTS

Based on Figure 1, the total number of patients recruited in this studywas191 patients. As many as97 and 94 subjects were analyzed in the AHF and CPL group, respectively. Each group had subjects who could not continue the intervention because of a failure to follow up. The baseline characteristics of patients are summarized in Table 1.

Table 1: Demographic data of patients.

Parameters	AHF (N=97)	CPL (N=94)
Mean age	45-55 yr	45-55 yr
Male:female	1.9:1	1.7:1
BMI (Overweight:normoweight)	1.18:1	1.38:1
History of recurrent urolithiasis	1 yr (34%)	1 yr (33%)
Average size of stone	10.82±8.19	8.07±5.19

Comparing male and female participants between the two groups were 1.9:1 and 1.7:1 in the AHF and CPL group, respectively. Each group also had a similar BMI ratio between overweight and normoweight participants. The majority of patients were in the range of 45-55 years old. About 30% of patients had a history of stone recurrence within one year before the study started. The mean of the size of the stone was similar between the two groups. Figure 2A shows information about the mean of the eGFR for pre-treatment(day 0) and post-treatment(day 56). There was no significant difference in the eGFR between the two groups on day 0. However, after 56 days of treatment, there were significant differences in the eGFR between the AHF group and the CPL group (p=0.044, 95% CI 0.16 – 12.4).

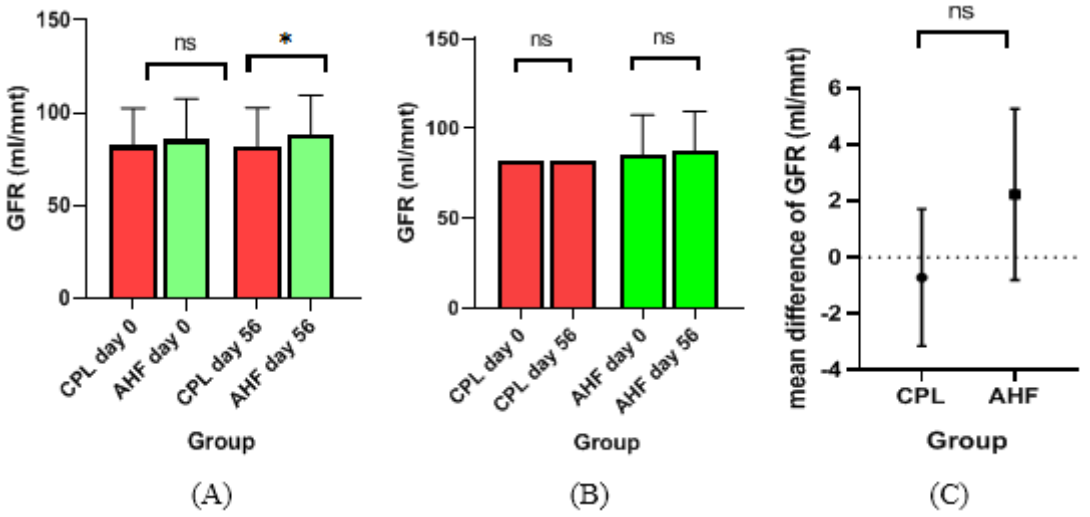

Figure 2: (A) Mean of eGFRfor pre- and post-treatment between the two groups.(B)Mean difference between AHF and CPL groups. (C)Mean of eGFR before and after treatment in each group.

An increase in subjects' eGFR was found in the AHF group on day 56 compared with day 0 (2.24 mL/min per 1.73 m2). However, this was not statistically significant (p=0.35). In the CPL group, the average eGFR of subjects on day 56 was lower than on day 0, though this was also not statistically significant (p=0.56) (Figure 2B). We calculated the difference in theeGFR value between day 0 and day 56 in each group, as represented in figure 2C. The difference in the eGFR in the AHF group showed a positive value, while in the CPL group, it showed a negative one.

However, the independent T-test analysis showed no significant differences. Table 2 shows the urine test parameters of subjects. These results demonstrate that both groups' urine turbidity had lower scores at the end of treatment than in the middle or baseline. There was a statistically significant difference during treatment compared to the baseline.

Furthermore, the CPL group's urine turbidity had substantial differences in the middle of treatment compared to the baseline. From the table, we can also see that there is no change in any other urine test parameter (pH, specific gravity, LE, Nitrite, RBC, or albuminuria).

4 DISCUSSION

This study was conducted to the potential renoprotective effect of an anti-urolithiasis herbal formula in urolithiasis patients. The eGFR Anti-urolithiasis Herbal Formula's group has a significant

Table 2: Effect of treatment on urine test parameters.

Parameters	AHF			CPL		
	day 0	day 28	day 56	day 0	day 28	day 56
Urine turbidity	1.95 ± 0.08	1.80 ± 0.08[a]	1.62±0.0 [a]p<0.05 [b]p<0.05	1.88 ± 0.08	1.73 ± 0.07 [a]p<0.05	1.68±0.07 [b]p<0.05
Urine pH	5.90 ± 0.09	6.74 ± 0.76	6.47 ± 0.57	5.97±0.096	6.02 ± 0.09	6.01 ± 0,09
Specific gravity	1.014±0.001	1.016±0.002	1.013±0.001	1.000±0.02	1.015±0.02	1.014±0.02
LE	82.55±16.41	74.64±15.85	72.73±15.90	92.02±17.95	91.76±18.06	87.04±18.09
Nitrite	0.04±0.02	0.03±0.02	0.04 ±0.02	0.08 ±0.03	0.05 ± 0.02	0.03 ± 0.02
No.of RBC's perHPF	59.10± 9.65	51.01±8.96	53.19±9.42	48.39±8.55	36.83±7.49	36.94±7.66
Albuminuria	20.57 ±3.75	16.94±3.71	17.89±4.05	16.40±2.52	14.84±2.50	12.83±2.20

Mean±SEM, Statistical analysis performed using independent T-test
[a] As compared to day0
[b] As compared to day 28

difference in day 56 after treatment compared to the CPL group. However, other parameters have not a significant difference in both groups. Furthermore, after urolithiasis formation, the hindrance of urine flow can cause a decrease in the Glomerular Filtration Rate (GFR). Therefore, waste material, especially BUN (Blood Urea Nitrogen), creatinine, and uric acid, can be collected in the blood(Kaleeswaran *et al*., 2019). This study showed that the AHF and CPL had diuretic activity, preventing the elevation of these parameters. Following a previously published report, the improvement of the eGFR in the AHF group compared to the CPL group was correlated to decreased urinary stones size (Nisa and Astana, 2019).

Orthosiphon stamineus and *Phyllanthus niruri* L are indigenous medicines widely used in Indonesia(Nisa and Astana, 2018). Meanwhile, previous studies reported that the content of rosmarinic acid in *Orthosiphon stamineus* had nephroprotective effects in diabetic nephropathy. It may have conserved glomerular number loss(Almatar *et al*., 2014; Tavafi *et al*., 2011). However, this complex mechanism remains unclear, and the antioxidant properties of *Orthosiphon stamineus* may play a significant role in this process. The activation of s cellular oxidation process was associated with urolithiasis and chronic calculus pyelonephritis(Boonla, 2018; Ceban *et al*., 2016). The potential anti-urolithiasis activity of *Phyllantus niruri* plays an essential role in the early stages of stone formation. *Phyllanthus niruri*can makes stones smoother and more fragile, facilitating the dissolution of calculi (Lee *et al*., 2016).

On the other hand, most of the AHF's constituents' main activity is as a diuretic agent. In terms of diuretic action, various phytoconstituents may interact with a synergistic effect, leading to enhanced renal output. The AHF treatment was revealed to increase the GFR by dual effects of controlling the growth of stones and may also have a nephroprotective effect. The renoprotective strategies of the AHF are based on several mechanisms and are exceedingly complex. Meanwhile, the antioxidant and anti-inflammatory effects of AHF may contribute to the preservative effects of microcirculation.

The present study results show the proportion of subjects who had a history of recurrence, the rate of which was 33%. Meanwhile, the ordinary recurrence rate of kidney stone disease within one year is only 10%(Patankar *et al*., 2020). Indeed, the high recurrency of urolithiasis disease was closely correlated with side effects, leading to renal function loss progression. Various degrees of renal insufficiency is associated with urolithiasis as well. This phenomenon suggests that a combination of frequent stone episode recurrence, urinary tract reinfection, and frequent urological interventions may initiate renal insufficiency. Many studies have found that urine parameters could serve as predictive factors for estimating renal function. One of the key biomarkers of renal damage is albuminuria. Several studies have reported that this decreases the risk of renal damage and urine albumin levels(Abebe *et al*., 2019). Albuminuria is a dysfunctional endothelial marker in the renal region, brain, and heart (Mardiana *et al*., 2012). Thus, anti-albuminuria was a target for the renoprotective agent. Remuzi and Bertani suggested that albuminuria was a severity marker for renal injury, indicating that an increase in leak plasma protein is associated with an increase in kidney damage severity (De Zeeuw *et al*., 2004). Several theories attempt to explain how urolithiasis can induce renal progression. Several mechanisms underlying nephrolithiasis can lead to CKD development through scarring and the deterioration of renal function. This phenomenon may also cause direct damage to post-calcifications and crystallization of the tubular lumen, resulting from recurrent stone obstruction (D'Costa *et al*., 2016).

The limitation of this study is the parameters of renal function, which used an estimated calculation. It still needs further research for real renal function parameters.

5 CONCLUSIONS

Our findings suggest that AHF has a slight potential effect on renal function preservation in urolithiasis patients.

ACKNOWLEDGEMENTS

This study was a part of the Saintifikasi Jamu formula (SJ) program that was carried out with the Ministry of Health's financial support of the Republic of Indonesia. We would like to thank the Head of B2P2TOOT in Tawangmangu, Indonesia, and all staff.

REFERENCES

Abebe, M., Adane, T., Kefyalew, K., Munduno, T., Fasil, A., Biadgo, B., *et al*., 2019. Variation of Urine

Parameters among Diabetic Patients: A Cross-Sectional Study. *Ethiop. J. Health Sci.* 29, 877–86. doi:10.4314/ejhs.v29i1.9

Adam, Y., Somchit, M.N., Sulaiman, M.R., Nasaruddin, A.A., Zuraini, A., Bustamam, A.A., *et al*., 2009. Diuretic properties of Orthosiphon stamineus Benth. *J. Ethnopharmacol.* doi:10.1016/j.jep.2009.04.014

Agawane, S.B., Gupta, V.S., Kulkarni, M.J., Bhattacharya, A.K., Koratkar, S.S., Rao, V.K., 2019. Patho-physiological evaluation of Duranta erecta for the treatment of urolithiasis. *J. Ayurveda Integr. Med.* 10, 4–11. doi:10.1016/j.jaim.2017.08.001

Ahmed, S., Hasan, M.M., Alam, Z., 2016. Antiurolithiasis plants in different countries and cultures. *J. Pharmacogn. Phytochem.* 5, 102–15.

Akane, W., Tsujihata, M., Yoshioka, I., Nonomura, N., Okuyama, A., 2010. Orthosiphon grandiflorum has a protective effect in a calcium oxalate stone-forming rat model. *Urol. Res.* 38, 89–96. doi:10.1007/s00240-010-0265-6

Alexander, R.T., Hemmelgarn, B.R., Wiebe, N., Bello, A., Morgan, C., Samuel, S., *et al*., 2012. Kidney stones and kidney function loss: a cohort study. *BMJ* 345, e5287. doi:10.1136/bmj.e5287

Almatar, M., Ekal, H., Rahmat, Z., 2014. A Glance on Medical Applications of Orthosiphon stamineus and Some of its Oxidative Compounds. *Int. J. Pharm. Sci. Rev. Res.* 24, 83–8.

Boonla, C., 2018. Oxidative Stress in Urolithiasis, in: Reactive Oxygen Species (ROS) in Living Cells. pp. 129–58. doi:10.5772/intechopen.75366

Ceban, E., Banov, P., Galescu, A., Botnari, V., 2016. Oxidative stress and antioxidant status in patients with complicated urolithiasis. *J. Med. Life* 9, 259–62.

Coe, F.L., Evan, A.P., Worcester, E.M., Lingeman, J.E., 2010. Three pathways for human kidney stone formation. *Urol. Res.* 38, 147–60. doi:10.1007/s00240-010-0271-8

D'Costa, M., Savcic-Kos, R., Huang, J., Rule, A.D., Murali, N., 2016. Urological procedures in urolithiasis and their association with chronic kidney disease. *Clin. Med. Res.* 14, 75–82. doi:10.3121/cmr.2016.1261

De Zeeuw, D., Remuzzi, G., Parving, H.H., Keane, W.F., Zhang, Z., Shahinfar, S., *et al*., 2004. Proteinuria, a target for renoprotection in patients with type 2 diabetic nephropathy: Lessons from RENAAL. *Kidney Int.* 65, 2309–20. doi:10.1111/j.1523-1755.2004.00653.x

E., K.A., J., L.A., E., P.D., T., G.M., 2008. Long-Term Outcomes of Percutaneous Nephrolithotomy Compared to Shock Wave Lithotripsy and Conservative Management. *J. Urol.* 179, 2233–7. doi:10.1016/j.juro.2008.01.115

Evan, A.P., 2010. Physiopathology and etiology of stone formation in the kidney and the urinary tract. *Pediatr. Nephrol.* 25, 831–41. doi:10.1007/s00467-009-1116-y

Giribabu, N., Karim, K., Kilari, E.K., Salleh, N., 2017. Phyllanthus niruri leaves aqueous extract improves kidney functions, ameliorates kidney oxidative stress, inflammation, fibrosis and apoptosis and enhances kidney cell proliferation in adult male rats with diabetes mellitus. *J. Ethnopharmacol.* 205, 123–37. doi:10.1016/j.jep.2017.05.002

Kaleeswaran, B., Ramadevi, S., Murugesan, R., Srigopalram, S., Suman, T., Balasubramanian, T., 2019. Evaluation of anti-urolithiasis potential of ethyl acetate extract of Pedalium murex L. on struvite crystal (kidney stone). *J. Tradit. Complement. Med.* 9, 24–37. doi:10.1016/j.jtcme.2017.08.003

Khan, A., Bashir, S., Khan, S.R., Gilani, A.H., 2011. Antiurolithic activity of Origanum vulgare is mediated through multiple pathways. *BMC Complement. Altern. Med.* doi:10.1186/1472-6882-11-96

Lee, N.Y.S., Khoo, W.K.S., Adnan, M.A., Mahalingam, T.P., Fernandez, A.R., Jeevaratnam, K., 2016. The pharmacological potential of Phyllanthus niruri. *J. Pharm. Pharmacol.* 68, 953–69. doi:10.1111/jphp.12565

Lee, S.K., Kim, Y., Kang, H.W., Kim, W.T., Kim, Y., Yun, S., *et al*., 2015. Age and gender-associated metabolic characteristics of urinary stone patients. *J. Biomed Res.* 16, 172–6.

Mardiana, Kartini, A., Widjasena, B., 2012. Media Medika. *Pemberian Cairan Karbohidrat Elektrolit, Status Hidrasi dan Kelelahan pada Pekerja Wan.* 46, 6–11.

Morán, E., Budía, A., Broseta, E., Boronat, F., 2013. Phytotherapy in urology. Current scientific evidence of its application in urolithiasis, chronic pelvic pain, erectile dysfunction and urinary tract infections. *Actas Urológicas Españolas (English Ed.* 37, 174–80. doi:10.1016/j.acuroe.2012.07.016

Nisa, U., Astana, P.R.W., 2019. Evaluation of Antiurolithic Herbal Formula for Urolithiasis: a Randomized Open-Label Clinical Study. *Asian J. Pharm. Clin. Res.* 12, 88–93. doi:10.22159/ajpcr.2019.v12i4.30232

Nisa, U., Astana, P.R.W., 2018. Studi Etnofarmakologi Tumbuhan obat untuk Mengobati Gangguan Batu Saluran Kemih di Sumatera Indonesia. *Bul. Penelit. Kesehat.* 46, 275–86.

Nizami, A.N., Rahman, M.A., Ahmed, N.U., Islam, M.S., 2012. Whole Leea macrophylla ethanolic extract normalizes kidney deposits and recovers renal impairments in an ethylene glycol-induced urolithiasis model of rats. *Asian Pac. J. Trop. Med.* 5, 533–8. doi:10.1016/S1995-7645(12)60094-7

Patankar, S.B., Mujumdar, A.M., Bernard, F., Supriya, P., 2020. Safety and efficacy of an herbal formulation in patients with renal calculi - A 28 week, randomized, double-blind, placebo-controlled, parallel-group study. *J. Ayurveda Integr. Med.* 11, 62–7. doi:10.1016/j.jaim.2018.08.001

Shekar Kumaran, M.G., Patki, P.S., 2011. Evaluation of an Ayurvedic formulation (Cystone), in urolithiasis: A double-blind, placebo-controlled study. *Eur. J. Integr. Med.* 3, 23–8. doi:10.1016/j.eujim.2011.02.003

Srisubat, A., Potisat, S., Lojanapiwat, B., Setthawong, V., Laopaiboon, M., 2014. Extracorporeal shock wave lithotripsy (ESWL) versus percutaneous nephrolithotomy (PCNL) or retrograde intrarenal surgery (RIRS) for kidney stones. *Cochrane Database*

Syst. Rev. 2014. doi:10.1002/14651858.CD007044.pub3

Tavafi, M., Ahmadvand, H., Khalatbari, A., Tamjidipoor, A., 2011. Rosmarinic acid ameliorates diabetic nephropathy in uninephrectomized diabetic rats. *Iran. J. Basic Med. Sci.* 14, 275–83. doi:10.22038/ijbms.2011.5006

Tiwari, P., Kothiyal, P., Ratan, P., 2017. Antiurolithiasis Effect of Some Polyherbal Formulations Used in Experimentally Induced Urolithiasis: a Review. *Int. Res. J. Pharm.* 8, 14–22. doi:10.7897/2230-8407.08566

Yadav, RD., Jain, SK., Alok, Shashi., Mahor, Alok., Bharti, JP., Jaiswal, M., Yadav D, R., Jain S, K., Alok, S., Mahor, A., Bharti P, J., *et al*., 2011. Herbal Plants Used in The Treatment of Urolithiasis: A Review. *Int. J. Pharm. Sci. Res.* 2, 1412–20.